Sensors and Actuators B 177 (2013) 848–855

Contents lists available at SciVerse ScienceDirect

Sensors and Actuators B: Chemical

journal homepage: www.elsevier.com/locate/snb

Microneedle biosensor: A method for direct label-free real time protein detection

Rahim Esfandyarpour[a,b,*], Hesaam Esfandyarpour[a], Mehdi Javanmard[b], James S. Harris[a], Ronald W. Davis[b]

[a] Center for Integrated Systems, Department of Electrical Engineering, Stanford University, USA
[b] Stanford Genome Technology Center, 855 California Ave., Palo Alto, CA 94304, USA

ARTICLE INFO

Article history:
Received 21 July 2012
Received in revised form
17 November 2012
Accepted 19 November 2012
Available online 7 December 2012

Keywords:
Impedance sensing
Microfluidics
Biosensing
Nanoneedle
Nanotechnology
Protein detection
Protein array
Label-free detection

ABSTRACT

Here we present the development of an array of electrical micro-biosensors in a microfluidic channel, called microneedle biosensors. A microneedle biosensor is a real-time, label-free, direct electrical detection platform, which is capable of high sensitivity detection, measuring the change in ionic current and impedance modulation, due to the presence or reaction of biomolecules such as proteins and nucleic acids. In this study, we successfully fabricated and electrically characterized the sensors and demonstrated successful detection of target protein. In this study, we used biotinylated bovine serum albumin as the receptor and streptavidin as the target analyte.

1. Introduction

Low cost detection of biomolecular has various applications in medicine, biotechnology and can potentially enable the dream of personalized medicine [1]. Biomolecules of interest may range from proteins [2], nucleic acids [3], whole cells [4], and metabolites [5]. Most biosensors fall under the following categories: calorimetric, electrical, optical, and mechanical. The most common techniques for optical detection include fluorescence detection [6], surface plasmon resonance (SPR), surface enhanced Raman spectroscopy (SERS) [7], colorimetric for color and photometric for light intensity [8]. The most common techniques for mechanical detection include scanning probe microscopy (SPM) [9], atomic force microscopy (AFM) [10], scanning tunneling microscope (STM) [11], and quartz crystal microbalance (QCM) [12]. Piezo-electric devices typically use gold to detect the specific angle at which electron waves are emitted when the substance is exposed to laser light or crystals, such as quartz, which vibrate under the influence of an electric field [13,14]. Common techniques for electrical detection include impedance spectroscopy, potentiometry [17], and amperometry. Amperometric systems detect current resulting from movement of electrons in redox reactions detected when a potential is applied between two electrodes. Potentiometric systems detect change in the distribution of charge using ion-selective electrodes [15,16]. Colorimetric biosensors measure the change in light absorption, whereas photometric sensors measure light intensity or photon output from a luminescent or fluorescent process with photomultiplier tubes, charge coupled detectors, or similar systems [18]. For calorimetric biosensors, if the enzyme catalyzed reaction is exothermic, a temperature-sensitive resistor (thermistor) or thermocouple may be used to measure the reaction event [19]. For differential measurement, where the common noise can be reduced, the difference in the resistances, where one is exposed to the reaction but the reference sensor is not, represents the heat signal between reactant and product and hence, the analyte concentration. Various electrochemical biosensors have been developed for detection of biomolecules, such as DNA hybridization, DNA sequencing, protein or small molecule detection. For instance, for DNA hybridization, this can be accomplished by monitoring the hybridization of target DNA to probe DNA molecules which are attached to the surface of a sensor and measuring the change in conductance or double-layer capacitance resulting from hybridization of the probe and target DNA [20,21]. One class of electrical biosensors is impedance biosensors, which show promise for point-of-care and other applications [22–34]. Label-free detection has also been achieved using micro-scale impedance sensing [35].

* Corresponding author at: Center for Integrated Systems, Department of Electrical Engineering, Stanford University, USA. Tel.: +1 650 387 5976.
E-mail address: rahimes@stanford.edu (R. Esfandyarpour).

0925-4005/$ – see front matter © 2012 Elsevier B.V. All rights reserved.
http://dx.doi.org/10.1016/j.snb.2012.11.064

Impedance biosensors are low cost, easy to miniaturize, and label-free.

2. Microneedle biosensor: concept

Here we present a novel microneedle biosensor used as an ultra-sensitive, real time, label-free and localized device, which shows promise to overcome some of the current limitations of biosensors. By real time, we refer to the ability to directly measure biomolecular binding as a function of time, which causes changes in the impedance measured. This can be useful for measuring reaction kinetic constants for various biomolecular species. This paper outlines the study of fabrication and testing results of the device. This sensor has the potential of measuring molecular interactions between small numbers of molecules, potentially down to a single molecule interaction, and is useful for the detection of biomarkers such as proteins or nucleic acids. A schematic of the device is shown in Figs. 1 and 2. There are two different possible microneedle structures; a horizontal microneedle structure (Fig. 1a) and a vertical nanoneedle structure (Fig. 2). In addition to achieving low cost and high sensitivity while being label-free, the other potential advantage of the microneedle structure is the ability to measure protein levels directly in vivo inside a living cell, due to its rigid solid-state structure while being thin at the same time. Potentially a thin functionalized needle can be inserted into a living cell, and impedance measurements can be made directly as proteins are binding onto the needle surface. This can be used for many different applications such as measuring protein expression for the purposes of drug screening. In this manuscript, we focus primarily on demonstrating a proof of concept using the horizontal microneedle structure, since it is easier to fabricate. While the horizontal structure is advantageous due to ease of fabrication, the vertical structure will likely offer advantages of higher transducer sensitivity, due to smaller sensing area. The other advantage of the vertical needle is that for future in vivo studies, it will be easier to load the cell of interest onto the needle compared to the horizontal structure. The results here demonstrate the utility of the horizontal microneedle structure for low cost label-free detection; however, these studies are also useful because the results obtained here can also be used as guidelines when designing the vertical nanoneedle structure.

The vertical nanoneedle biosensor structure consists of four layers. First, a metallic core needle which is surrounded by an oxide layer. The oxide layer is also surrounded by another metallic layer, which serves as the second electrode. The most out layer is an oxide layer to protect the outer electrode from the electrolyte. In Fig. 2c, we show results of finite element modeling simulations we have performed using COMSOL, where we simulate the changes in impedance at the tip of the vertical nanoneedle sensor as a result of protein binding. We model the protein binding to the sensor tip as several insulative cylindrical objects attached to the surface. The dimensions of the needle were the following: the inner metallic core has a radius of 30 nm, the surrounding insulator has a thickness of 20 nm, the outer metallic core has a thickness of 7 nm, and the outer insulative layer has a thickness of 15 nm. The proteins binding were represented as 10 nm diameter and 10 nm tall cylinders. These are rough representations of clusters of proteins binding.

We also examine a horizontal structure which effectively behaves similarly to the vertical structure, however it is easier to fabricate, thus we pursued fabrication of this structure instead of the vertical. The horizontal microneedle structure consists of three thin-film layers. There are two conductive layers with an insulator layer in between. There may be a protective oxide layer above or below the sensors to prevent the exposure of conductive electrodes to the solution. Underneath the bottom electrode, there is an oxide layer, which can be a thermally grown oxide, to insulate the first electrode from the substrate. Various thicknesses and geometrical designs have been fabricated and tested. For one of the sensors tested, the thickness of each electrode is 100 nm, and the middle oxide layer thickness is 20–30 nm. The top protective oxide layer thickness is 200 nm and the bottom oxide layer thickness is 250 nm (Fig. 1b). The width of the microneedle tip is 5 μm. The probe molecule (e.g. DNA molecule or protein) is immobilized on the tip of the microneedles. The binding of target molecules to the probe molecules modulates the impedance between the electrodes.

3. Microneedle biosensor advantages

Most electrical biosensors offer the advantage of real-time and label-free measurements; however they suffer from low sensitivity and low signal to noise ratio (SNR) due to ambient noise. One of the most important issues in biosensor development is specificity and detector sensitivity. The devices suffer from low SNR caused by different noise sources such as electrical, thermal noise, flicker (1/f), Johnson–Nyquist noise, fluidic fluctuations. On the other hand, the signal generated due to a reaction or binding event of a target molecule to a probe molecule is not large enough and needs to be amplified. Due to miniaturization of the microneedle tip, this device has potentially high sensitivity for the detection of small numbers of molecules. The sensing area of this sensor is a sub-micron sized area. Ultimately, by scaling this sensing area to approach the size of the biomolecule of interest one can potentially achieve single molecule detection. Binding of just a few molecules at the sensing area generates a signal, which could be detectable by the microneedle sensor device. This results in a high sensitivity detection limit. Another advantage of the microneedle biosensor is the scalability and ease of multiplexing. This is a very important feature to enable high throughput large scale proteomics and genomics. Since the sensing region is the small area at the tip of the sensor, the microneedle structure is much less sensitive to environmental perturbation and disturbance. In addition, since the proposed sensor can be configured and fabricated in a free-standing "needle" structure, it can potentially be used to be injected into and monitor/characterize the inside of a living cell. Due to its suspended rigid microstructure, the injection through the cell membrane can be envisioned. This may have substantial use in drug discovery.

4. Sensor fabrication

Here, we briefly explain the process for the fabrication of the horizontal microneedle biosensor. We performed the following steps in order to fabricate the biosensor devices. Starting out with an undoped silicon wafer (Fig. 3a), first, 250 nm of silicon oxide was thermally grown (Fig. 3b) on a silicon substrate. This was followed by the deposition of 100 nm of poly-silicon (Fig. 3c) using low pressure chemical vapor deposition (LPCVD), which was then doped with phosphorus to achieve a sheet resistance of 210 ohms per square. A 30 nm-thick SiO_2 layer was thermally grown (Fig. 3d) on the bottom p^+-silicon layer. Another 100 nm p^+-silicon layer was deposited again using LPCVD (Fig. 3e). Finally a 200 nm SiO_2 layer was deposited on top of the p^+-silicon layer (Fig. 3f) using plasma enhanced chemical vapor deposition (PECVD). We patterned the microneedle bundles by etching the 200 nm top-SiO_2 layer, 100 nm top p^+-silicon layer, and 30 nm middle oxide layer down to bottom p^+-silicon layer (Fig. 3g). We performed wet etch step to etch out the channel below the bundle of microneedles (Fig. 3h). Then we performed focus ion beam to expose the tips of the microneedles to the electrodes. Afterwards, we performed another etch step to expose the bonding pads to allow wire bonding. Fig. 4 shows an optical micrograph of a bird's eye view of our sensor. Then a premade microfluidic PDMS chip with a micro-channel in the bottom

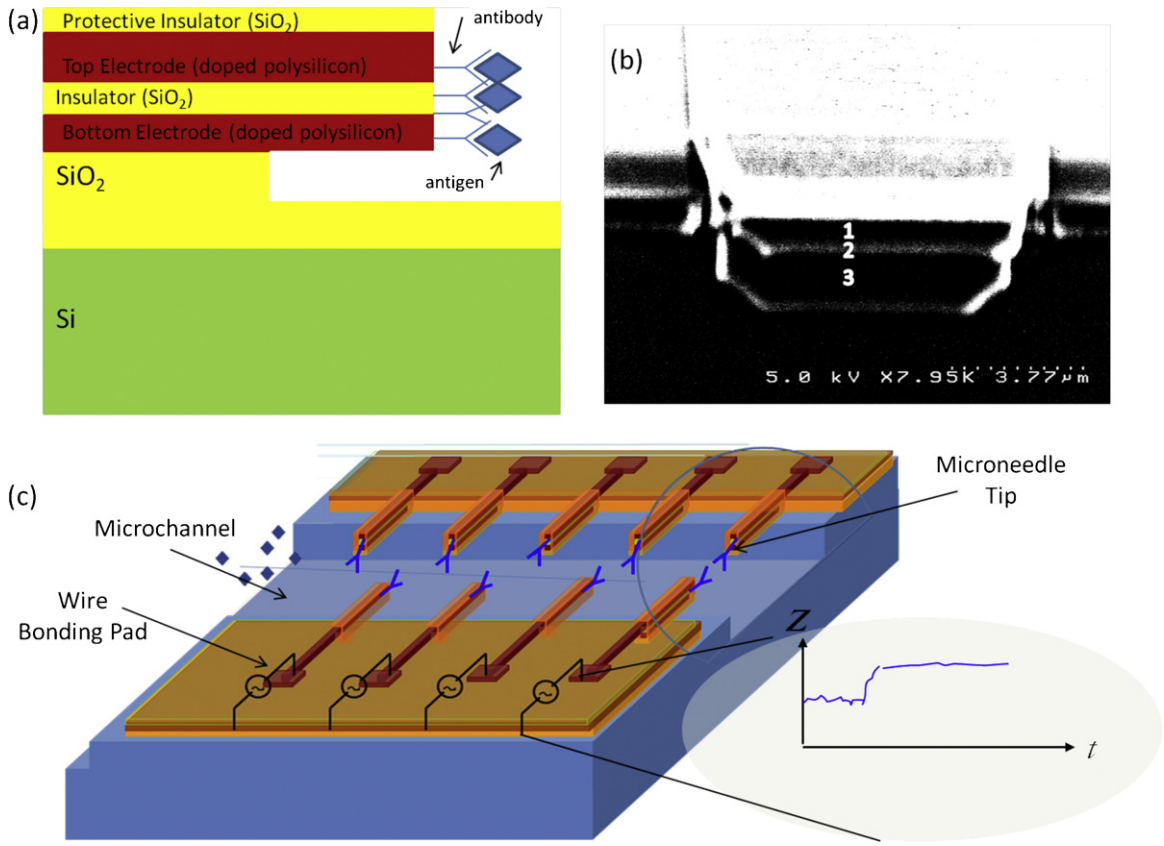

Fig. 1. (a) Schematic of microneedle biosensor side view of horizontal nanoneedles (not to scale), (b) SEM image of the tip of a microneedles biosensor; 1 and 3 are the electrodes; 2 is the oxide in between the electrodes, and (c) schematic of an array of horizontal microneedle biosensor in the channel.

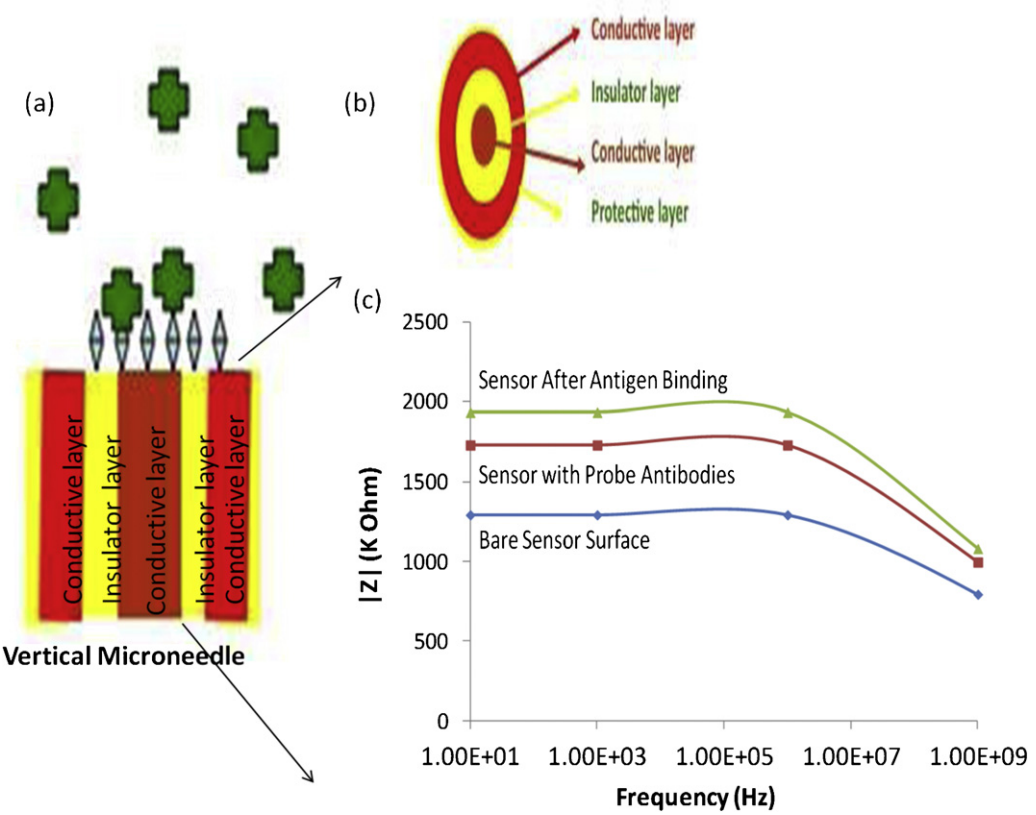

Fig. 2. (a) Side view schematic of a vertical nanoneedle biosensor. (b) Birds eye view schematic of vertical nanoneedles. (c) Finite element simulation result of impedance modulation for vertical nanoneedles as proteins bind to surface.

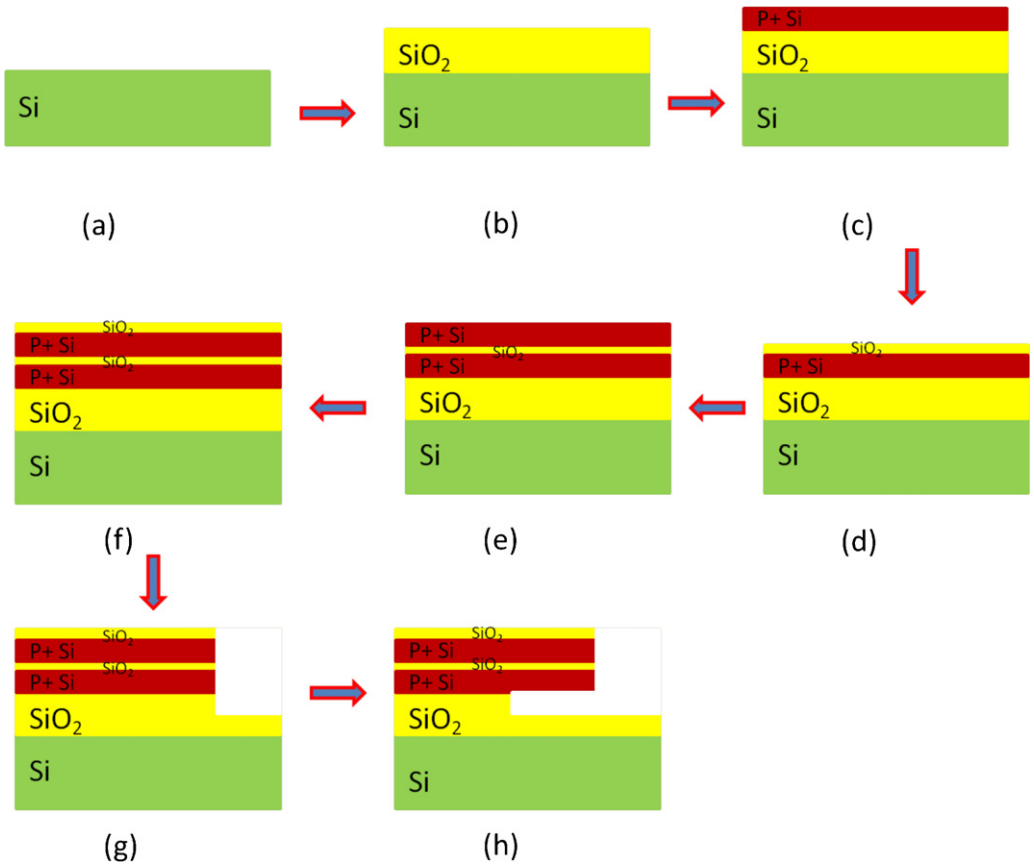

Fig. 3. Flow diagram of process for fabrication of microneedle biosensor.

of the device was bound to the substrate of the sensor channels using thermal bonding.

5. Measurements methods

Different methods such as amperometric, voltammetric, or impedance sensors have been used for the electrical measurements. For the voltammetry and amperometry methods the current at one electrode is measured as function of an applied electrode-solution voltage. These two approaches are DC, which causes a change in the properties at the surface of the electrode if the voltage applied is large enough. On the other hand, impedance biosensors can measure the electrical impedance of an interface using an AC steady state at lower voltage

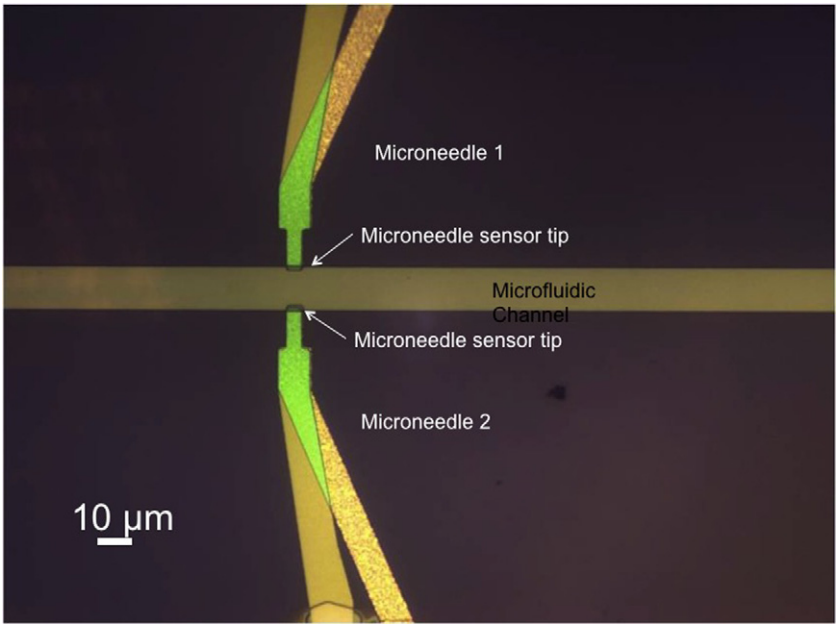

Fig. 4. Optical micrograph of a fabricated microneedles sensor from bird's eye view.

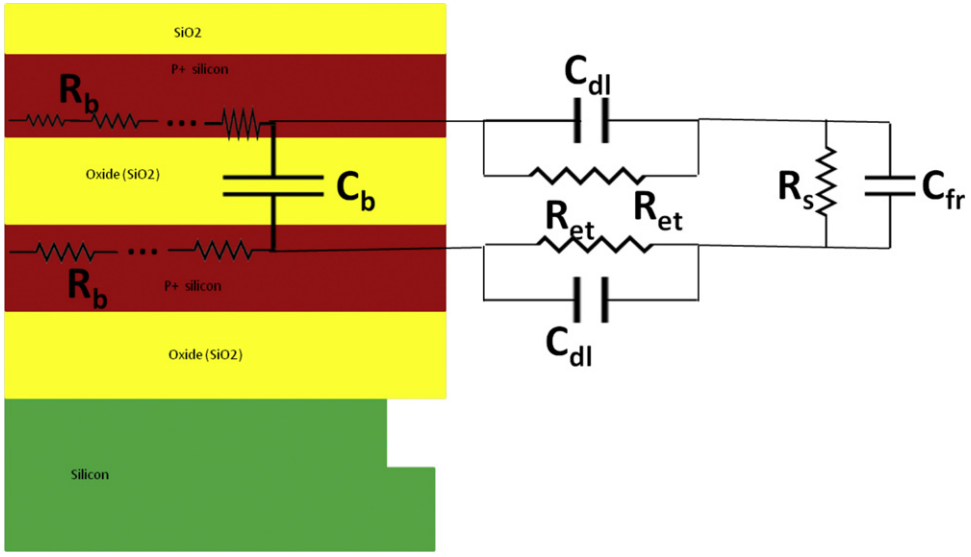

Fig. 5. Circuit diagram of parasitic resistances (solution resistance: R_s, body resistance: R_b, electron transfer resistance: R_{et}) and capacitances (double layer capacitance: C_{dl}, fringing capacitance: C_{fr}, body capacitance: C_b) of microneedle biosensor.

values. Electrochemical impedance spectroscopy (EIS) has been used to study a variety of electrochemical phenomena over a wide frequency range or a single frequency. A voltage excitation is commonly applied in electrochemical impedance spectroscopy (EIS). The measured electrode-solution impedance and the various parasitic impedances are in parallel in EIS. Fig. 5 shows a schematic of the circuit model of our microneedles senor's parasitic resistances and capacitances where the solution resistance is represented by R_s, the needle body resistance is represented by R_b, the electron transfer resistance is represented by R_{et}, the double layer capacitance is represented by C_{dl}, the fringing capacitance is represented C_{fr}, and the body capacitance is represented by C_b. The AC voltage or AC current can be applied while the other variable is measured. Applied voltage signal can be defined as below:

$$V_{applied} = V_{DC} + V_{AC}\ \sin(\omega t)$$

The resulting current would be:

$$I_{applied} = I_{DC} + I_{AC}\ \sin(\omega t - \theta)$$

The magnitude of the measured electrical impedance, $Z(\omega)$, is the ratio of V_{AC} over I_{AC}, and its phase is θ. The electrode solution impedance depends on two factors: bias conditions and the measurement frequency. Here we need to excite our device with a single frequency; for this purpose a "lock-in amplifier" is one of the options, which can be used to accurately measure the output signal at the same frequency. When the target analyte binds to the sensitive area of the sensor, the impedance of the electrode solution interface changes. The change in the impedance is a function of the number of antigens that bind to the microneedles surface, which is a function of the concentration of target molecules in the test sample. Electrochemical impedance spectroscopy can be used for detection of that impedance change. For several reasons the applied voltage should be small during the impedance measurements. First, linearity of the current–voltage relationship for the device is accurate only for small modulations, due to the fact that the size of the electrical double layer at the surface changes with large enough voltages. Avoiding modifying or disturbing of the probe layer due to electrolysis is the second reason. We tested microneedle biosensor devices for protein detection by using biotinylated BSA and streptavidin as the analytes. Electrochemical impedance spectroscopy (EIS) is used for the impedance measurements, as described in the next section.

6. Sensor characterization and experimental results

In order to perform EIS measurements on the microneedle biosensor we used a Versa STAT3 potentiostat (Princeton Instruments, Princeton, New Jersey). A sinusoidal voltage signal was applied to the top electrodes and the current entering the bottom electrode was measured and used to calculate the impedance. The measured impedance consists of different elements such as bulk capacitance, bulk resistance, fringing capacitance, double layer capacitance, double layer resistance and solution resistance. By applying a voltage between two electrodes; a current passes through the solution. The ratio of the applied voltage to the passing current gives the value of the impedance of the device. We measured the impedance spectrum from 0.1 Hz to 1 MHz. Our measurements show that the optimal frequency at which maximum change in measured impedance occurs due to biomolecular binding is between 1 and 10 kHz. The first pole in our system occurs at 100 kHz. This means that changes which we see in impedance resulting from binding is due to changes in the Debye layer capacitance. Above 100 kHz, the electrolyte bulk resistance dominates the impedance. Ideally for our system, maximum changes would occur

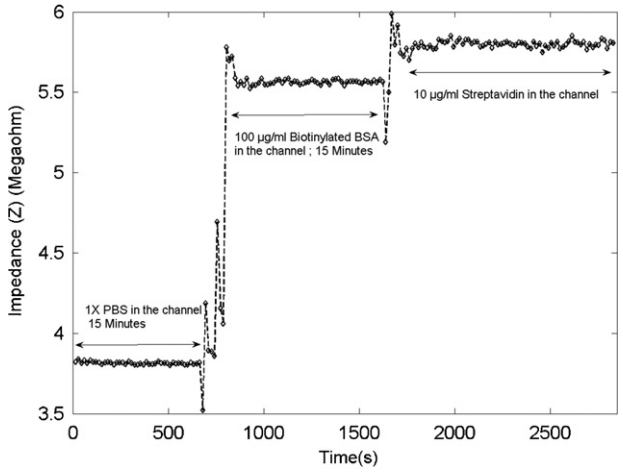

Fig. 6. Impedance measurement vs. time. BSA suspended in PBS at a concentration of 100 µg/ml and streptavidin solution at a concentration of 10 µg/ml.

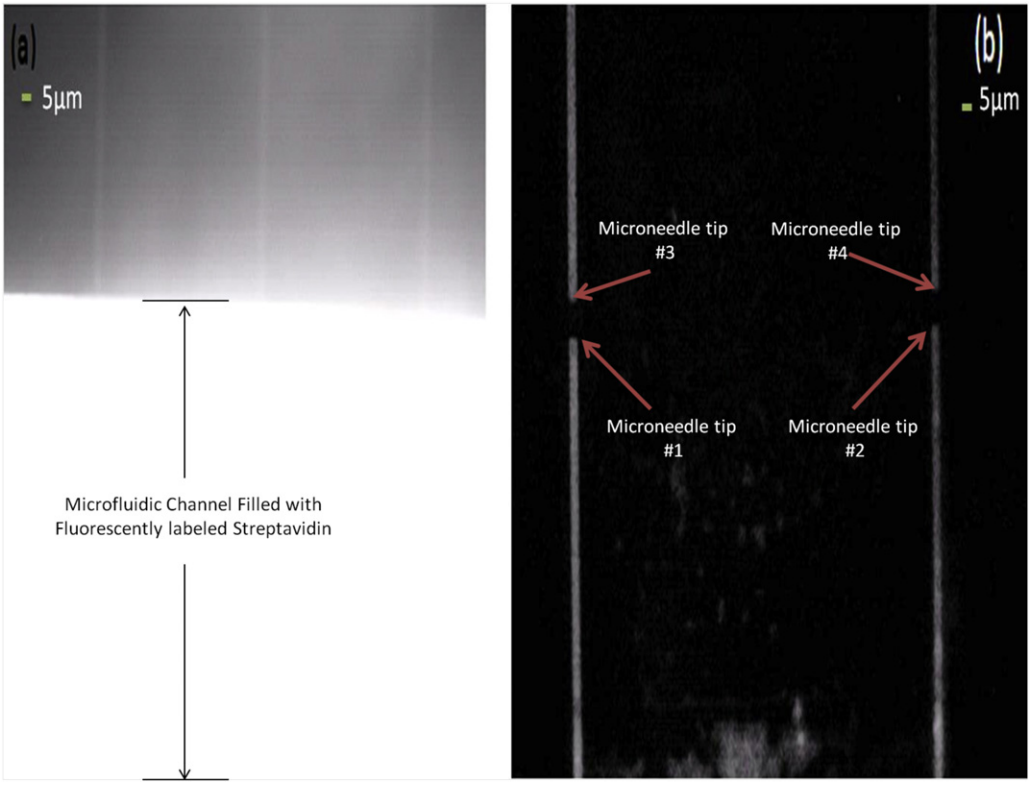

Fig. 7. (a) The microchannel is full of fluorescently labeled streptavidin. The microneedle tips are not visible since they are buried in the channel which is full of fluorescently labeled streptavidin. (b) The channel after the unbound streptavidin has been washed out. Fluorescently labeled streptavidin molecules are bound to the biotinylated BSA molecules attached on the surface of the needle. There are four separate microneedles in figure b, which we have labeled and shown with arrows. One thing to note is that figure b is shifted upward compared to figure a. In figure b, the border of the microchannel is off the picture.

in lower frequencies (<1 kHz), however the reason why changes below 1 kHz are not seen is due to the small size of the sensor tip resulting in a very small double layer capacitance at the interface resulting in a very high interfacial impedance (>100 GΩ) of our sensor at low frequencies. This results in much higher noise in our potentiostat, compared to the frequency range, which we worked with. This makes working in the 1–10 kHz range more practical for our sensing purposes, because the magnitude of the impedance is lower which makes it easier to measure with our potentiostat instrument. From here on, for the real time measurements, a 100 mV RMS 10 kHz AC signal is applied.

7. Protein detection

In order to show the proof of concept for protein detection with microneedle devices, we tested the ability of our sensors to detect binding of biotin and streptavidin in real time. Biotinylated BSA–streptavidin binding was chosen to demonstrate the effectiveness of device functionality. This binding has been extensively studied and is a well understood process, and therefore can serve to model and characterize a system for protein interactions. The procedure for this experiment is as follows: phosphate buffer saline (PBS) was injected into the channel and the impedance was measured. This impedance is the baseline of all the measurements. All the changes can be compared to this base line. The next step was incubation for 15 min to allow the solution to reach a steady state. Then, biotinylated BSA (bovine serum albumin) molecules, which act as receptor proteins, were injected into the microchannel. This protein physically adsorbs and binds to the oxide surface. The biotinylated BSA solution was suspended in PBS at a concentration of 100 μg/ml. It took less than a minute to reach steady state. Afterwards, as a control, while the impedance was being monitored, PBS was injected into the channel to ensure that the changes in impedance are not spurious and are due to molecules attaching to the surface. This resulted in no change in impedance beyond the noise level. Streptavidin was then injected into the channel. Streptavidin was resuspended in PBS at a concentration of 10 μg/ml.

After a few seconds streptavidin molecules started to bind to the surface-attached biotinylated BSA molecules. Fig. 6 shows representative data of a typical binding curve over time. The binding of the streptavidin molecules to the biotinilated BSA results in about a 5% change in impedance.

As a control, we injected PBS into the channel and measured the impedance. The change of impedance after this washing step was insignificant to the extent that it was buried in noise. It shows that the measured impedance is only modulated when a molecule is bound to the sensor active area, resulting in a change of impedance. The measured impedance changes are not due to unbound streptavidin molecules or changes in electrolyte conductivity. These experiments were repeated three times, and the same exact trend was observed.

One thing to note is that the change in impedance as a result of streptavidin binding is not as large compared to the change in impedance when biotinilated BSA binds to the surface, although in terms of size they are both on the same order of magnitude. This is to be expected, because the streptavidin is farther away from the electrode surface relative to the BSA, thus having less interaction with the Debye layer compared to BSA.

We assumed first order Langmuir kinetics for simplicity and using the following equation:

$$\frac{b_{eq}}{b_m} = \frac{C_0/K_D}{1+(C_0/K_D)}$$

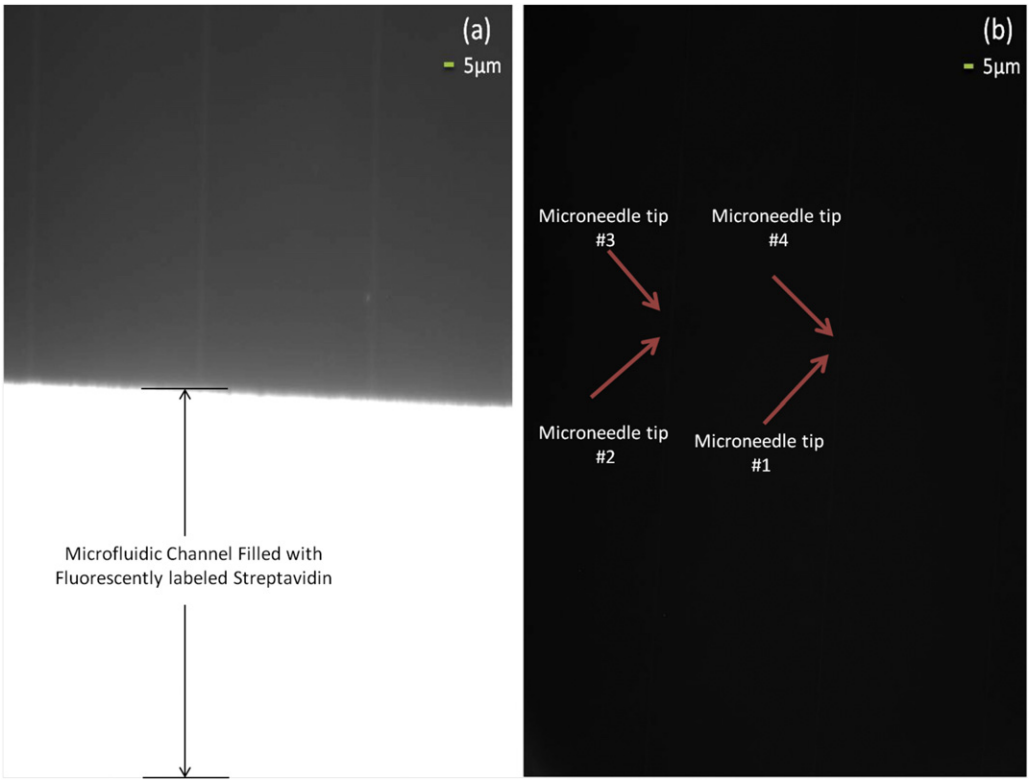

Fig. 8. (a) Immobilized non biotinylated BSA molecules are bound to the surface of the sensor. The microchannel is full of fluorescently labeled streptavidin. The microneedle tips are not visible since they are buried in the channel which is full of fluorescently labeled streptavidin. (b) The same channel after washing out with 1× PBS. No fluorescently labeled streptavidin molecule is still bound. The arrow points to the tips of the needle, which is very dim due to the fact that the fluorescent streptavidin molecules have not bound to the needle surface. There are four separate microneedles in figure b. One thing to note is that figure b is shifted upward compared to figure a. In figure b, the border of the microchannel is off the picture.

where b_{eq} is the number of molecules bound to the sensor surface in equilibrium, b_m is the number of probe molecules attached to the sensor surface (where we assumed 1×10^{10} probe molecules per cm^2 and an active sensing area of 24.2 μm^2, C_0 is the concentration of streptavidin molecules in the bulk (130 nM), and K_D is the affinity constant of streptavidin biotin binding (10^{-14} M). Using this equation and assuming that we are operating in the reaction limited regime, we calculated that approximately 2400 molecules have bound to the surface sensor.

8. Control experiments

Two control experiments were performed to confirm that the change of impedance was due to specific binding of streptavidin molecules to the biotinylated BSA molecules. For the first control experiment biotinylated BSA molecules were used as the receptors and fluorescently labeled streptavidin molecules were used as the target proteins. The experimental steps were exactly the same as the previous experiment. Biotinylated BSA was injected into the channel and incubated for 15 min. The channel was washed with PBS, and then fluorescently-labeled streptavidin was injected into the channel. Fig. 7a shows the channel full of fluorescently labeled streptavidin molecules. The channel was very bright because the channel was full of fluorescently labeled streptavidin molecules before any washing took place. Then the channel was washed with PBS and another image of the sensors in the channel was captured. As seen in Fig. 7b fluorescently labeled streptavidin molecules were bound to the surface-attached biotinylated BSA molecules on the surface of the needle.

For the other control experiment, we immobilized regular non-biotinilated BSA molecules to the surface of the sensor. We expected no fluorescently labeled streptavidin molecules to bind. As we expected all fluorescently labeled streptavidin molecules were removed from the channel after washing (Fig. 8). There was no biotin linked to the BSA molecules and thus no binding occurred. These control experiments confirmed that the electrical signal shown in Fig. 4 was due to the specific protein binding.

9. Conclusion

We have presented the design, simulation, fabrication, and testing of microneedle biosensors for protein detection. The results demonstrated the feasibility of potentially using microneedle biosensors for detection of biomolecular interactions. As already mentioned, electronic sensing using microneedle biosensors devices offers several advantages. These sensors are small, fast, and the active detection area may be sized for detection of individual proteins or viruses. The needles can potentially be used for large scale multiplexed cancer biomarker discovery. Microneedle biosensors can be designed and fabricated in a pixel array format as an integrated and localized biosensor, with the possibility of arrays of hundreds of micro-sensors per square millimeter of a device. Because of the use of electrical detection, we envision the application of these sensors in an integrated handheld system for point of care clinical diagnostics.

Acknowledgement

This work was supported by the National Institutes of Health grant PO1HG000205.

References

[1] M.A. Hamburg, F.S. Collins, New England Journal of Medicine 363 (301) (2010).
[2] H. Zhu, M. Snyder, Current Opinion in Chemical Biology 5 (40) (2001).
[3] M. Schena, D. Shalon, R.W. Davis, P.O. Brown, Science 270 (467) (1995).
[4] J.B. Smerage, D.F. Hayes, British Journal of Cancer 94 (8) (2006).
[5] J.B. German, M.A. Roberts, S.M. Watkins, Journal of Nutrition 133 (2003) 2078–2083.
[6] P.S. Dittrich, A. Manz, Analytical and Bioanalytical Chemistry 382 (2005) 1771–1782.
[7] G.L. Liu, L.P. Lee, Applied Physics Letters 87 (2005) 074101.
[8] A.K. Ellerbee, S.T. Phillips, A.C. Siegel, K.A. Mirica, A.W. Martinez, P. Striehl, N. Jain, M. Prentiss, G.M. Whitesides, Analytical Chemistry 18 (2009) 8447.
[9] L.A. Bottomley, Analytical Chemistry 70 (425R) (1998).
[10] S. Husale, H.H. Persson, O. Sahin, Nature 462 (2009) 1075.
[11] G. Binnig, H. Rohrer, C. Gerber, E. Weibel, Surface Science 131 (1983) L379.
[12] C.K. O'sullivan, G.G. Guilbault, Biosensors and Bioelectronics 14 (663) (1999).
[13] X. Zhou, L. Liu, M. Hu, L. Wang, J. Hu, Journal of Pharmaceutical and Biomedical Analysis 27 (341) (2002).
[14] J.M. Abad, F. Pariente, L. Hernández, H.D. Abruña, E.L. Pariente, Analytical Chemistry 70 (1998) 2848.
[15] M.S. Belluzo, M.E. Ribone, C.M. Lagier, Sensors 3 (2008) 1366.
[16] T. Ikeda, K. Kano, Journal of Bioscience and Bioengineering 92 (9) (2001).
[17] A.A. Karyakin, O.A. Bobrova, L.V. Lukachova, E.E. Karyakina, Sensors and Actuators B: Chemical 33 (1996) 34.
[18] C. Wang, Z. Ma, T. Wang, Z. Su, Advanced Functional Materials 16 (2006) 1673.
[19] S. Vermeir, B.M. Nicolaï, P. Verboven, P. Van Gerwen, B. Baeten, L. Hoflack, V. Vulsteke, J. Lammertyn, Analytical Chemistry 79 (2007) 6119.
[20] H. Cai, Y. Wang, P. He, Y. Fang, Analytica Chimica Acta 469 (165) (2002).
[21] J.J. Gooding, Electroanalysis 14 (2002) 1149.
[22] S. Basuray, S. Senapati, A. Aijian, A.R. Mahon, H.C. Chang, ACS Nano 3 (2009) 1823.
[23] J.S. Daniels, N. Pourmand, Electroanalysis 19 (2007) 1239.
[24] M. Gębala, W. Schuhmann, ChemPhysChem 11 (13) (2010).
[25] A. Bonanni, I. Fernández-Cuesta, X. Borrisé, F. Pérez-Murano, S. Alegret, M. Valle, Mikrochimica Acta 170 (275) (2010).
[26] G. Zhang, R. Zhu, Electroanalysis 22 (3) (2010).
[27] J.K.R. Kendall, B.R.G. Johnson, P.H. Symonds, G. Imperato, R.J. Bushby, J.D. Gwyer, C. van Berkel, S.D. Evans, L.J.C. Jeuken, ChemPhysChem 11 (10) (2010).
[28] X. Chen, Z. Guo, G.-M. Yang, J. Li, M.-Q. Li, J.-H. Liu, X.-J. Huang, Materials Today 13 (28) (2010).
[29] T. Ignat, M. Miu, I. Kleps, A. Bragaru, M. Simion, M. Danila, Materials Science and Engineering B 169 (55) (2010).
[30] Rajesh, V. Sharma, V.K. Tanwar, S.K. Mishra, A.M. Biradar, Thin Solid Films 519 (2010) 1167.
[31] B.-Y. Chang, S.-M. Park, Electrochemical Impedance Spectroscopy, Annual Review of Analytical Chemistry 3 (207) (2010).
[32] B. Lindholm-Sethson, J. Nyström, M. Malmsten, L. Ringstad, A. Nelson, P. Geladi, Analytical and Bioanalytical Chemistry 398 (2010) 2341.
[33] S. Cunningham, J.Q. Gerlach, M. Kane, L. Joshi, The Analyst 135 (2010) 2471.
[34] B. Su, J. Tang, J. Huang, H. Yang, B. Qiu, G. Chen, D. Tang, Electroanalysis 22 (22) (2010).
[35] C. Ionescu-Zanetti, J.T. Nevill, D. Di Carlo, K.H. Jeong, L.P. Lee, Journal of Applied Physics 99 (1) (2006).

Biographies

Rahim Esfandyarpour obtained his B.S. with the honor from K.N. Toosi University of Technology (2007), Tehran, Iran. He has joined Stanford in 2008 where he got M.S. degree in Electrical Engineering (2010) and he is pursuing his Ph.D. in Electrical Engineering from Stanford University, CA, USA. Since he started his graduate study in Electrical Engineering department, he joined Stanford Genome Technology Center and Nanobiotechnology Projects there. His main research areas are biosensors, bioelectronics, nanotechnology, and microfluidics with an emphasis on protein biomarkers and genetic biomarkers.

Dr. Hesaam Esfandyarpour is the inventor of electronic DNA sequencing through pH or heat detection. He developed the technology during his Ph.D. work, culminating in his thesis entitled "Electronic Gene Sequencing: A novel method for DNA sequencing based on direct heat or pH measurement" at the Stanford Genome Technology Center and the Center for Integrated Systems at Stanford University. The label-free and fast electronic sequencing technology results to dramatically reduce the cost of sequencing, in both instrumentation and running costs. Dr. Esfandyarpour founded GenapSys, Inc., a biotechnology company developing a fully integrated genetic analysis product, where he serves as CEO and Chief Technology Officer. Hesaam obtained a B.Sc. (with honors) from Sharif University, a M.Sc. in Electrical Engineering, a M.Sc. in Management Science and Engineering, and a Ph.D. in Electrical Engineering from Stanford University in 2004, 2006, 2008 and 2010 respectively. He was appointed as a Genome Fellow at the world renowned Stanford Genome Technology Center. Dr. Esfandyarpour has several publications and is the inventor or co-inventor of numerous patents and pending patents related to DNA sequencing and protein detection technologies.

Mehdi Javanmard received his BS degree with highest honors from the Georgia Institute of Technology in 2002, and the MS degree from Stanford University in 2004, and the PhD degree from Stanford University in 2008 all in Electrical Engineering. He has held research positions in Georgia Tech Research Institute, Lawrence Livermore National Laboratory, Stanford Linear Accelerator Center, and Stanford Genome Technology Center. His main research areas are biosensors, bioelectronics, and microfluidics with an emphasis on detection of pathogenic bacteria, genetic biomarkers, and protein biomarkers. He is currently an Engineering Research Associate at Stanford University.

James Harris is the James and Ellenor Chesebrough Professor of Electrical Engineering, Applied Physics and Materials Science at Stanford University. He received B.S., M.S. and Ph.D. degrees in Electrical Engineering from Stanford University in 1964, 1965 and 1969, respectively. In 1969, Dr. Harris joined the Rockwell International Science Center in Thousand Oaks, CA where he initiated much of their work on III–V compound semiconductors. He was one of the key contributors in developing ion implantation in GaAs, MBE and heterojunction device technologies, leading to Rockwell's preeminent position in GaAs device technology. He was successively Manager of infrared devices, Principal Scientist and Director of the Optoelectronics Research Department. In 1982, Dr. Harris joined the Solid State Electronics Laboratory, Stanford University, as Professor of Electrical Engineering to establish a program in compound semiconductor materials and heterojunction devices. His current research interests are in the physics and application of ultra-small structures and novel materials to new optoelectronic devices, interconnect and biosensors. He has supervised over 95 PhD students and has over 850 publications in these areas. Dr. Harris is a Fellow member of the National Academy of Engineering and Material Research Society of IEEE, the American Physical Society, Optical Society of America and he received the 2000 IEEE Morris N. Liebmann Award, the 2000 International Compound Semiconductor Conference Welker Medal, an IEEE Third Millennium Medal and an Alexander von Humboldt Senior Research Prize in 1998 and the 2008 international MBE conference MBE innovator award.

Prof. Ronald W. Davis received the BS degree in Mathematics, Physics, Chemistry, and Botany from East Illinois University in 1964, and the PhD in Chemistry from California Institute of Technology in 1970. He is considered to be a world leader in biotechnology, and the development and application of recombinant DNA and genomic methodology to biological systems. His laboratory has developed many of the techniques currently used in academic and industrial biotechnology laboratories. He is also considered to be a world expert in the electron microscopy of nucleic acids and has developed many of the mapping methods for which he received the Eli Lilly Award in Microbiology in 1976. His laboratory was also instrumental in the development of lambda vectors, which were commonly used for the primary cloning of DNA molecules in *E. coli*. His laboratory also developed many of the yeast vectors and helped to develop yeast as a host for recombinant DNA for which he received the United States Steel Award in 1981, presented by the National Academy of Sciences. In 1983 he became a member of The National Academy of Sciences. He was a co-author on a publication that first described a new approach for conducting human genetics and for the construction of a human genetic linkage map for which he received the Rosentiel Award for Work in Basic Medical Research. His laboratory is now conducting genomic analysis of *Saccharomyces cerevisiae* for which he received the 2004 Lifetime Achievement Award from the Yeast Genetics Society. His laboratory is developing many new technologies for the genetic, genomic, and molecular analysis of model organisms and human with a focus on clinical medicine for which he received the 2004 Sober Award from the American Society for Biochemistry and Molecular Biology (ASBMB/IUBMB).